

Technical Communication

Upper-bound finite-element analysis of axisymmetric problems using a mesh adaptive strategy

Jian Zhang^a, Yufeng Gao^a, Tugen Feng^{a,*}, Junsheng Yang^b, Feng Yang^b^a College of Civil and Transportation Engineering, Hohai University, Nanjing, Jiangsu 210098, China^b School of Civil Engineering, Central South University, Changsha, Hunan 410075, China

ARTICLE INFO

Keywords:

Axisymmetric examples
Equivalent plane strain
Power dissipation
Upper-bound finite-element method
Adaptive strategy

ABSTRACT

A plastic-dissipation-based mesh adaptive algorithm is first introduced into the upper-bound finite-element method to determine the stability of axisymmetric problems using an equivalent plane strain model. The failure loads for two geotechnical examples were presented in the form of dimensionless stability numbers. The refined meshes and power dissipations were also plotted to highlight evolutionary characteristics of failure mechanisms. Comparisons are given to verify the effectiveness of the mesh adaptive strategy. The advantage of the present method lies in the improved accuracy of the upper-bound solution and the ability to provide failure patterns with greater clarity.

1. Introduction

Various limit analysis approaches, such as finite-element-based methods [1–10], boundary-element-based methods [11,12], and element-free-based methods [13,14], have been proved to be effective tools for evaluating the stability of engineering structures. Among these methods, the finite-element limit analysis method is the most popular because of its effectiveness and simplicity. In the past few decades, limit analysis has been used to solve geotechnical stability problems for plane strain cases, and only a few attempts have been undertaken to analyze axisymmetric stability problems. With the help of nonlinear programming, Lyamin and Sloan [15] and Lyamin et al. [16] investigated the failure loads of axisymmetric problems using a three-dimensional (3D) finite-element limit analysis formulation. Later, Krabbenhøft et al. [17] and Martin and Makrodimopoulos [18] provided convenient frameworks for performing limit analysis of 3D structures using semidefinite programming. In this method, the flow rule and power dissipation are expressed in the form of principal strains, and the yield criterion can be expressed in the form of principal stresses. However, on account of extensive computation and inherent challenges, the solving procedure remains challenging to perform relative to the process of solving the plane strain problem. To reduce the computational effort, some studies have considered the axisymmetric stability problem using an equivalent plane strain model [19–23]. Pastor and Turgeman [19] and Turgeman and Pastor [20] introduced $3p$ inequality constraints for each element in the formulations to perform upper- and lower-bound limit analysis of equivalent plane strain

problems, where p is the sum of sides of the polygon used to linearize the Mohr-Coulomb yield criterion. Relative to the plane strain case, these formulations require an additional $2p$ inequality constraints for each element. Later, Chakraborty and Kumar [22] investigated the axisymmetric problems for materials following the Drucker-Prager yield criterion. The circumscribed/inscribed truncated icosahedrons are applied to replace the 3D form of the Drucker-Prager yield criterion. Moreover, based on the Haar and von Karman hypothesis [24], Kumar and Khatri [20] and Kumar and Chakraborty [23] introduced $p + 3$ inequality constraints for each element in the formulations instead of the $3p$ inequality constraints required in the study by Turgeman and Pastor [20]. In this approach, the hoop stress is kept close to either the major principle compressive stress or the minor principle compressive stress.

For axisymmetric stability problems with equivalent plane strain models, the combination of constant strain elements (three-node elements) and velocity discontinuities is preferred to discretize these analysis models. However, as overestimating the incompressibility of three-node elements in the formulation, the accuracy of results is strongly affected by the number and layout of elements. Here, based on the Haar and von Karman hypothesis [24], an upper-bound finite-element method in combination with a plastic-dissipation-based mesh adaptive strategy and linear programming is employed to investigate the stability numbers and corresponding failure patterns of axisymmetric problems for materials following the Mohr-Coulomb yield criterion. We show through two geotechnical examples that upper-bound solutions with fine accuracy can be obtained by automatically refining

* Corresponding author.

E-mail address: fengtugen@hhu.edu.cn (T. Feng).

the failure regions with high strain rates, especially for large friction angles. Moreover, an improved failure mechanism that can exhibit the evolutionary characteristics of slip lines is also presented. The results are compared with those available in the literature using various numerical methods.

2. A brief review of the upper-bound finite-element method for axisymmetric problems

The rigorous theoretical foundation of the upper-bound finite-element method makes it suitable for determining the stability of geotechnical structures. The formulations for axisymmetric problems originate from those proposed by Kumar and Chakraborty [23]. The domain in an r - z plane is applied for analysis of the equivalent plane strain problem. Nodal velocities, plastic multiplier rates and auxiliary variables of velocity discontinuities are all treated as unknown variables to be investigated during the solution procedure. The velocity variables changed linearly in each element, and discontinuous velocity fields were permitted among the elements. To establish a linear programming model, a regular p -side polygon is applied to linearize the Mohr-Coulomb yield criterion, which must be inscribed to the polygon. An upper bound on the collapse load can be obtained by minimizing the internal power dissipation minus the rate of work done by external forces subjected to: (i) equality constraints generated from the satisfaction of (a) plastic flow both within elements and along velocity discontinuities, and (b) velocity boundary conditions; and (ii) inequality constraints arising from (a) the linearization of the yield criterion and (b) the elimination of the nonlinear expressions generated from the imposition of constraints along velocity discontinuities.

Compared with plane strain problem, no difference is generated in the axisymmetric formulation when applying constraints along velocity discontinuities and velocity boundaries. These relative formulations are explained in detail in Sloan and Kleeman [1]. However, the constraints arising from the imposition of the associated flow rule within elements are different because of the introduction of the Haar-von Karman hypothesis, which states that the circumferential stress $\sigma_\theta = \sigma_1$ (maximum compressive normal stress) in an active case and that $\sigma_\theta = \sigma_3$ (minimum compressive normal stress) in a passive case. The correctness of the Haar-von Karman hypothesis has been confirmed [25,26], and this hypothesis has been shown to be a natural consequence in combination of the associated flow rule and the Mohr-Coulomb yield criterion [27]. With reference to Fig. 1, except for those originating from the Mohr-Coulomb yield criterion, three additional inequality yield constraints are defined to ensure the restriction on σ_θ in the presented constraints. For the case that the soil mass is in an active state of failure, the three expressions can be cast in the following form:

$$F_{p+1} = \sigma_\theta - \sigma_r \leq 0 \tag{1a}$$

$$F_{p+2} = \sigma_\theta - \sigma_z \leq 0 \tag{1b}$$

$$F_{p+3} = \sigma_{1f} - \sigma_\theta \leq 0 \tag{1c}$$

In addition, for the passive case:

$$F_{p+1} = \sigma_r - \sigma_\theta \leq 0 \tag{2a}$$

$$F_{p+2} = \sigma_z - \sigma_\theta \leq 0 \tag{2b}$$

$$F_{p+3} = \sigma_\theta - \sigma_{3f} \leq 0 \tag{2c}$$

where $(\sigma_r, \sigma_z, \sigma_\theta)$ are normal stresses along the direction of the axes; $(\sigma_{1f}, \sigma_{3f})$ are the maximum and minimum normal stresses at failure.

The linear programming model can be cast in the following form:

$$\text{Minimize } \sum_{i=1}^{n_d} P_{d,i} + \sum_{i=1}^{n_e} P_{p,i} + \sum_{i=1}^{n_e} P_{e,i} \tag{3}$$

Subject to

$$\left\{ \begin{aligned} \dot{\epsilon}_{r,i} &= \frac{\partial u}{\partial r} = \sum_{m=1}^{p+3} \lambda_{m,i} \frac{\partial F_{m,i}}{\partial \sigma_{r,i}} = \sum_{m=1}^p \lambda_{m,i} A_{m,i} + \dot{\lambda}_{p+1,i} \frac{\partial F_{p+1,i}}{\partial \sigma_{r,i}} \\ &+ \dot{\lambda}_{p+2,i} \frac{\partial F_{p+2,i}}{\partial \sigma_{r,i}} + \dot{\lambda}_{p+3,i} \frac{\partial F_{p+3,i}}{\partial \sigma_{r,i}} \quad (i = 1, \dots, n_e) \\ \dot{\epsilon}_{z,i} &= \frac{\partial v}{\partial z} = \sum_{m=1}^{p+3} \lambda_{m,i} \frac{\partial F_{m,i}}{\partial \sigma_{z,i}} = \sum_{m=1}^p \lambda_{m,i} B_{m,i} + \dot{\lambda}_{p+1,i} \frac{\partial F_{p+1,i}}{\partial \sigma_{z,i}} \\ &+ \dot{\lambda}_{p+2,i} \frac{\partial F_{p+2,i}}{\partial \sigma_{z,i}} + \dot{\lambda}_{p+3,i} \frac{\partial F_{p+3,i}}{\partial \sigma_{z,i}} \quad (i = 1, \dots, n_e) \\ \dot{\gamma}_{rz,i} &= \frac{\partial v}{\partial r} + \frac{\partial u}{\partial z} = \sum_{m=1}^{p+3} \lambda_{m,i} \frac{\partial F_{m,i}}{\partial \tau_{z,i}} = \sum_{m=1}^p \lambda_{m,i} C_{m,i} + \dot{\lambda}_{p+1,i} \frac{\partial F_{p+1,i}}{\partial \tau_{z,i}} \\ &+ \dot{\lambda}_{p+2,i} \frac{\partial F_{p+2,i}}{\partial \tau_{z,i}} + \dot{\lambda}_{p+3,i} \frac{\partial F_{p+3,i}}{\partial \tau_{z,i}} \quad (i = 1, \dots, n_e) \\ \dot{\epsilon}_{\theta,i} &= \frac{u}{r} = \sum_{m=1}^{p+3} \lambda_{m,i} \frac{\partial F_{m,i}}{\partial \sigma_{\theta,i}} = \sum_{m=1}^p \lambda_{m,i} D_{m,i} + \dot{\lambda}_{p+1,i} \frac{\partial F_{p+1,i}}{\partial \sigma_{\theta,i}} \\ &+ \dot{\lambda}_{p+2,i} \frac{\partial F_{p+2,i}}{\partial \sigma_{\theta,i}} + \dot{\lambda}_{p+3,i} \frac{\partial F_{p+3,i}}{\partial \sigma_{\theta,i}} \quad (i = 1, \dots, n_e) \\ \Delta u_{1,2,i} &= u_{1,2,i}^+ - u_{1,2,i}^- = (u_{2,i} - u_{1,i}) \cos \beta_i + (v_{2,i} - v_{1,i}) \sin \beta_i \quad (i = 1, \dots, n_d) \quad (e) \\ \Delta u_{3,4,i} &= u_{3,4,i}^+ - u_{3,4,i}^- = (u_{4,i} - u_{3,i}) \cos \beta_i + (v_{4,i} - v_{3,i}) \sin \beta_i \quad (i = 1, \dots, n_d) \quad (f) \\ \Delta v_{2,i} &= (u_{1,2,i}^+ + u_{1,2,i}^-) \tan \phi = (u_{1,i} - u_{2,i}) \sin \beta_i + (v_{2,i} - v_{1,i}) \cos \beta_i \quad (i = 1, \dots, n_d) \quad (g) \\ \Delta v_{3,4,i} &= (u_{3,4,i}^+ + u_{3,4,i}^-) \tan \phi = (u_{3,i} - u_{4,i}) \sin \beta_i + (v_{4,i} - v_{3,i}) \cos \beta_i \quad (i = 1, \dots, n_d) \quad (h) \\ u_i \cos \omega_i + v_i \sin \omega_i &= \bar{u}_i \quad (i = 1, \dots, n_v) \quad (i) \\ v_i \cos \omega_i - u_i \sin \omega_i &= \bar{v}_i \quad (i = 1, \dots, n_v) \quad (j) \end{aligned} \right. \tag{4}$$

where $P_{p,i} = 2\pi \bar{r}_{e,i} \int_{A_i} (\sigma_{r,i} \dot{\epsilon}_{r,i} + \sigma_{z,i} \dot{\epsilon}_{z,i} + \tau_{z,i} \dot{\gamma}_{rz,i} + \sigma_{\theta,i} \dot{\epsilon}_{\theta,i}) dA$ represents the power dissipated within the element, A^i is the area of the i^{th} element, $(\sigma_{r,i}, \sigma_{z,i}, \tau_{z,i}, \sigma_{\theta,i})$ define the normal and shear stresses of the i^{th} element, $(\dot{\epsilon}_{r,i}, \dot{\epsilon}_{z,i}, \dot{\gamma}_{rz,i}, \dot{\epsilon}_{\theta,i})$ are the normal and shear strain rates of the i^{th} element, and $\bar{r}_{e,i}$ is the distance between the centroid of the i^{th} triangle element and the z -axis; $P_{d,i} = 2\pi \bar{r}_{d,i} \int_{l_{d,i}} c_i |\Delta u_i| dl$ represents the power dissipated along the velocity discontinuity, c_i is the cohesion; Δu_i defines the tangential velocity jump for the i^{th} velocity discontinuity, $l_{d,i}$ is the length of the i^{th} velocity discontinuity, and $\bar{r}_{d,i}$ is the value of r at the central point of the i^{th} velocity discontinuity; $P_{e,i} = 2\pi \bar{r}_{e,i} (-\int_{A_i} \gamma_i v_i dA)$ is the power done by soil weight, γ_i is the unit weight, and v_i is the velocity for the i^{th} element in the horizontal-direction; and (n_d, n_e) are the total number of velocity discontinuities and elements, respectively.

Note that Eqs. (4a)–(4d) describe the flow rule in continuum; $F_{m,i}$ is composed of (i) the function for the m^{th} side of the yield polygon, (ii) additional inequality constraints shown in Eqs. (1) and (2); $\lambda_{m,i}$ represents a non-negative plastic multiplier rate; p is the total numbers of sides of the polygon that is applied to linearize the failure criterion; (u, v) are the velocities of an arbitrary point for an element in the horizontal- and vertical-directions; $(A_{m,i}, B_{m,i}, C_{m,i})$ are parameters

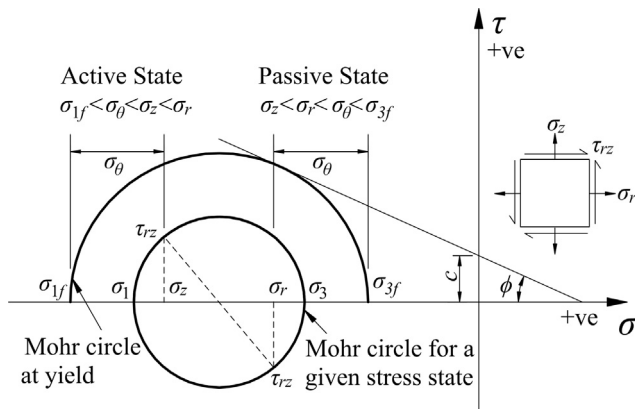


Fig. 1. Range of the circumferential stress σ_θ .

Download English Version:

<https://daneshyari.com/en/article/9951852>

Download Persian Version:

<https://daneshyari.com/article/9951852>

[Daneshyari.com](https://daneshyari.com)